HHS Public Access

Author manuscript

J Biomed Mater Res A. Author manuscript; available in PMC 2022 July 01.

Published in final edited form as:

J Biomed Mater Res A. 2021 July ; 109(7): 1080–1087. doi:10.1002/jbm.a.37100.

Sustained Delivery of VEGF from Mesoporous Calcium-deficient Hydroxyapatite Microparticles Promotes In Vitro Angiogenesis and Osteogenesis.

Charlotte Piard[1], **Rachel Lutchke**[1], **Timur Kamalitdinov**[1], **John Fisher**[1,2,*]

[1]Fischell Department of Bioengineering, University of Maryland, 3121 A. James Clark Hall, College Park, MD 20742, United States

[2]Center for Engineering Complex Tissues, University of Maryland, 3121 A. James Clark Hall, College Park, MD 20742, United States

Abstract

Promoting the growth of blood vessels within engineered tissues remains one of the main challenge in bone tissue engineering. One way to improve angiogenesis is the use of vascular endothelial growth factor (VEGF) as it holds the ability to increase the formation of a vascular network. In the present study, collagen scaffolds with VEGF-releasing hydroxyapatite particles were fabricated, in order to engineer a material both capable of presenting an osteoconductive surface and delivering an angiogenic growth factor in a localized and sustained manner, in order to enhance osteogenesis as well as angiogenesis. To this end, we developed microparticles and characterize their size, chemical properties and Ca/P ratio to validate the formation of hydroxyapatite. We then evaluated the osteogenic potential of HAp when cultured with mesenchymal stem cells (hMSCs) and compare it to commercially available hydroxyapatite (SBp). Finally, we characterized the encapsulation and release of VEGF in the HAp and assess the angiogenic potential of the VEGF-HAp when cultured with endothelial cells. We demonstrated the successful fabrication of calcium deficient hydroxyapatite microparticles (CDHAp), with biological properties closer to the bone than stoichiometric, commercially available hydroxyapatite. This CDHAp exhibited a well-defined 3D network of crystalline nanoplates forming mesoporous and hollow structures. The high specific area created by those structures enabled the loading of VEGF with high efficiency when compared to the loading efficiency of SBp. Furthermore, their biological performances were evaluated in vitro. Our results indicate that VEGF-CDHAp can be used to improve both osteogenesis and angiogenesis in vitro.

Keywords

Hydroxyapatite; Biomimetic; VEGF; Microparticles; Bone Tissue Engineering

[*]**Corresponding Author(s):** John P. Fisher, Fischell Family Distinguished Professor & Department Chair, Fischell Department of Bioengineering, University of Maryland, 4102A Clark Hall, 8278 Paint Branch Drive, College Park, MD 20742, Phone: 301.314.2188, jpfisher@umd.edu.

Introduction

Promoting the growth of blood vessels within engineered tissues remains one of the main challenge in bone tissue engineering [1]. A variety of approaches, including growth factors delivery, scaffold functionalization, material surface modification, and cell-based techniques, have been developed for this purpose. The delivery of vascular endothelial growth factor (VEGF) is a particularly promising way to enhance angiogenesis as it holds the ability to increase the formation of a vascular network [2], [3] resulting in increased blood flow.

Hydrogels are among the most commonly reported delivery systems for growth factors (GFs) but in some cases, they are unable to release GFs in a controlled and sustained manner for extended periods, and often show an initial burst release of the GFs [4], [5]. Moreover, uncontrolled delivery of growth factors can also lead to heterotopic tissue formation or hematomas in soft tissues. This occurs as a result of GFs fast release and diffusion into other areas of the body, due to the uncontrolled manner in which the GF is released [6]. Microparticles have emerged as a potent delivery system, that can entrap GFs while controlling their release [7], [8]. The scientific literature describes numerous techniques for encapsulating drugs in a variety of materials [9], [10]. To be used as a GFs carrier, the material forming the microparticles must have the ability to (i) incorporate a drug either physically or chemically, (ii) retain the drug, (iii) and in addition to diffusion, be gradually degraded to deliver the drug in a controlled manner over time [11]. Quinlan et al [10] used a two step methods to promote both vascularization and bone repair: (i) the encapsulation of VEGF in spray-dried alginate microparticles and (ii) the suspention of hydroxyapatite in a collagen scaffold. Combining both steps and using a material that is both osteoinductive and able to form particles in order to encapsulate VEGF would be ideal and novel. Calcium phosphates (CaP) met both those criteria.

Hydroxyapatite (HA), ($Ca_{10}(PO_4)_6(OH)_2$), is a form of CaP with a Ca/P ratio of 1.67. HA is widely used in bone tissue engineering due to its structural and chemical similarities with the key mineral component of bone [12]–[15]. HA is also used in chromatography for purification and separation as an absorbent agent to its excellent absorption of many molecules [16]. CaP systems are increasingly being explored as drug delivery systems for orthopedics over other ceramics: they are biocompatible, have bioaffinity, are osteoconductive and in certain cases, osteoinductive [17]. Porous hydroxyapatite microparticles (HAp) can be prepared according to a great diversity of methods, the simplest being chemical precipitation [18].

In the study described here, the overall objective was to enhance the regenerative capacity of tissue engineering scaffolds through the incorporation of therapeutic GFs. Specifically, collagen scaffolds loaded with VEGF-releasing hydroxyapatite particles, in an attempt to fabricate a scaffold capable of localizing and sustaining the release of VEGF over extended periods. We hypothesized that a scaffold presenting an osteoconductive surface and capable of delivering an angiogenic growth factor in a localized and sustained manner would enhance osteogenesis as well as angiogenesis. To this end, our first objective was to develop microparticles and characterize their size, chemical properties and Ca/P ratio to validate the formation of hydroxyapatite. Our second objective was to evaluate the osteogenic potential

of HAp when cultured with mesenchymal stem cells (hMSCs) and compare it to commercially available hydroxyapatite (SBp). Our final objective was to characterize the encapsulation and release of VEGF in the HAp and assess the angiogenic potential of the VEGF-HAp when cultured with endothelial cells.

Materials and Methods

Microparticles Synthesis and Characterization

Synthesis.—Calcium chloride anhydrous (CaCl2), sodium carbonate anhydrous (Na2CO3), disodium phosphate dodecahydrate (Na2HPO4·12H2O), aspartic acid (Asp), and sodium dodecyl sulfate (SDS) were purchased from Sigma (St. Louis, MO). Hydroxyapatite particles (HAp) were synthesized in a two-step reaction previously described elsewhere [19] (Figure Ia). Aspartic acid and sodium dodecyl sulfate were used as a surfactant to form hollow calcium carbonate (CaCO3) sacrificial template. HAp was then formed by an anion exchange process between CaCO3 and disodium phosphate dodecahydrate (Na2HPO4, 12H2O). Briefly, two solution were prepared: (i) 0.1 mol/L of CaCl2, 0.1 mol/L of Na2CO3 and 0.5 g/L of Asp, and (ii) 0.1 mol/L of CaCl2, 0.1 mol/L of Na2CO3, 0.5 g/L Asp and 30 mmol/L SDS. Calcuim carbonate crystals were formed by precipitation, mixing solution (i) into solution (ii), and stirring for 1 h at 40 °C. Afterward, an equal volume of 0.03 mol/L Na2HPO4–12H2O was added to the CaCO3 solution dropwise, and stirred at a constant rate of 200rpm, for 3h at 50 °C and pH10. After 3h, the collected particles were filtered, rinsed in distilled water and washed with ethanol. The particles were flash freeze in liquid nitrogen before being dried in a lyophilizer.

Microparticles morphology & size distributions.—The structure of the microspheres was investigated by field emission scanning electron microscopy (FE-SEM) (Hitachi SU-70, Japan). The particle size distributions were measured using a Mastersizer S apparatus (Malvern Instruments, United Kingdom), based on dynamic light scattering (DLS). For each analysis, 50 mg of particles were suspended in distilled water and their sizes and deviations was measured.

X-ray photoelectron spectroscopy (XPS).—The chemical composition of the particles and their calcium-phosphate ratio was measured using a high sensitivity Kratos AXIS 165 spectrometer (Kratos Analytical Ltd, United Kingdom).

X-ray powder diffraction (XRD)—patterns were measured under a Bruker Apex2 diffractometer (Brucker, Billerica, MA).

Cell Culture

RoosterBasal Media supplemented with RoosterBooster was used to culture hMSCs (RoosterBio, Frederick, MD), following manufacturer’s protocols. Cells were cultured on tissue culture polystyrene flasks for 5 days. Cells (P3) were passages once reached 90% confluency, using trypsin/EDTA. The osteogenic media was composed of growth media (Gibco, Carlsbad, CA) supplemented with 100nM dexamethasone (Sigma, St. Louis, MO), 10mM β-glycerophosphate, and 173 mM ascorbic acid (Sigma). HUVECs (P4) (Lonza)

were grown in EBM-2 Basal Medium (Lonza) supplemented by EGM-2 SingleQuot Kit. Both cell media was changed every 3 days.

Live/Dead Assay.—Cell viability was assessed using a Live/Dead assay (Invitrogen) using manufacturer protocols. HAp (2mg/ml) and hMSCs (1.10^6 cells/ml) were suspended in 4 mg/ml type I collagen (Corning) and scaffolds were formed by pipetting 150 μl of the cells/HAp/Collagen solution in a 12 wells plate and incubated 15 min at 37 °C to crosslink. After 24h culture in media, the scaffolds were incubated in 2 mM ethidium homodimer and 4 mM calcein AM (Molecular Probes) for 30 min. Fluorescent and brightfield images were then taken using an inverted microscope (Nikon Eclipse Ti2).

Growth factor loading and VEGF release study.

In vitro experiment to measure drug loading and release were performed. VEGF (Sigma) adsorption to HA was performed by incubating 2mg/ml HAp into a solution of 6ng/ml of VEGF (C0). Commercial available hydroxyapatite (<200nm) (SBp) (Sigma, St. Louis, MO) were used as a control. The solutions were then incubated at 37°C for 1 h on a shaker. After centrifugation, the VEGF-loaded microparticles (HAp or SBp) were dyhadrated at 24°C under a vacuum overnight. Samples of the supernatants were frozen for later analysis. The concentration of VEGF contained in the supernatant was determined by Enzyme-Linked Immunosorbent Assay (ELISA) (Abcam, Cambridge, MA). The VEGF-loaded samples were referred to as VEGF-HAp or VEGF-SBp.

The release rate of VEGF from the microparticles in an aqueous environment was measured. VEGF-HAp and VEGF-SBp were incubated with 1 mg of VEGF/mL for 1h, shaking at 37°C. At each timepoint, 200 μL of solution was removed from the vial and flash frozen for later analysis, and replace with an egal volume of PBS. After collecting all samples, the extracted PBS was analyzed using an ELISA (Abcam, Cambridge, MA) to determine VEGF concentration.

Osteogenic/Angiogenic Potential Experiments

For all experiments, 2mg/ml of particles (HAp or SBp) and 1.10^6 cells/ml were suspended in 4 mg/ml type I collagen (Corning) and scaffolds were formed by pipetting 150 μl of the cells/HAp/Collagen solution in a 12 wells plate. Scaffolds containing no hydroxyapatite were used as controls. For osteogenic experiments, hMSCs were used and cultured in osteogenic media for 14 days along with HAp or SBp. For angiogenic experiments, HUVECs were used and grown in growth media for 7 days, along with VEGF-HAp and VEGF-SBp.

DNA quantification Assay.—Scaffolds from each group (n=3) were collected after 0 and 7 days of culture (HUVECs) and 0 and 14 days of culture (hMSCs). Collagen hydrogels were dissolved in 2 mg/mL collagenase (Sigma) for 30 min at 37°C and the cells were isolated by centrifugation. Total DNA was isolated using DNeasy Blood and Tissue Kit (Qiagen) and DNA content was quantified using the PicoGreen DNA assay (Invitrogen), following the manufacturers protocols. An XTT (2,3-bis-(2-methoxy-4-nitro-5-

sulfophenyl)-2H-tetrazolium-5-carboxanilide) (Sigma) assay was performed, according to the manufacturer's protocol, at the same time point on all groups to quantify.

Quantitative Reverse Transcriptase Polymerase Chain Reaction (qRT-PCR).— After 0, 7 and 14 days (hMSCs) or 0 and 7 days (HUVECs) of culture, scaffolds from each group were collected. To isolate mRNA from the cells, the scaffolds were dissolved in collagenase (Sigma) for 30 min at 37°C and cells were collected by centrifugation. Total RNA was isolated and TaqMan Reverse Transcription Reagents (Applied Biosystems, Foster City, CA) was used to perform reverse transcription. qRT-PCR was performed using TaqMan PCR Master Mix and TaqMan Gene Expression Assays for the following genes: bone morphogenetic protein 2 (BMP2), osteocalcin (OCN), vascular endothelial growth factor A (VEGFA) and platelet endothelial cell adhesion molecule (PECAM). Quantification of target genes was performed relative to the housekeeping control gene GADPH. The mean minimal cycle threshold values (Ct) were obtained form three reactions.

Von Kossa Staining.—hMSCs scaffolds were cultured in osteogenic media for 14 days and then fixed in 4% paraformaldehyde (PFA) (Sigma) for 15 min. For histological analysis, the samples were dehydrated in successive ethanol washes (75%, 90%, 100%), and then embedded in paraffin (Fisher Scientific), and sectioned using a microtome (Leica) into 5-micron-thick sections. For the Von Kossa staining, 2.5% (w/v) silver nitrate (20 min under UV), 5% (w/v) sodium carbonate (5 min), and 0.1% Nuclear Fast Red (Poly Scientific) were used.

Migration Assay.—The scratch wound assay is a straighforward, rapid and cost-effective method to quantify ECs migration [20]. HUVECs were seeded in 48 well plates at a density of 30,000 cells per well, and incubated for 24h or until a uniform monolayer was formed. The monolayer was then "scratched" using a pipette tip to create a linear gap through the middle of each well. Growth medium supplemented with 0.5 mg/ml VEGF/HAp or 0.5 mg/ml VEGF/SBp were used. Full growth media was used as a positive control, while serum free media was used as a negative control. Images of the wells were taken using an inverted microscope (Nikon Eclipse Ti2) after 0h and 12h of incubation. Pictures were analyzed using ImageJ to determine the overall gap closure, as previously described [21].

Statistical Analysis.

All samples were evaluated in biological and technical triplicates. Data were analyzed using ANOVA and a Tukey's Multiple Comparison Test assuming normal data distribution with a confidence of 95% ($p<0.05$).

Results

Formation of Calcium Deficient Hydroxyapatite Microparticles (CDHAp)

Microparticles were measured to have an average diameter of 8.08 +/− 2.68 μm, with 96.35% of particles being between 5 μm and 20 μm (Figure Ib). SEM images of the particles (Figure Ic) show that homogeneous crystalloids were obtained. Commercially available particles (SBp) were also analyzed and were 73.8 +/− 15.6 nm in diameter. Some broken

microparticles can be observed revealing a hollow interior. The XRD patterns of the microparticles are presented in Figure Id. The diffraction peaks at 25.8°, 28.9°, 31.7°, 32.8°, 34.0°, 39.1°, 46.7°, 49.4°, and 53.2° matched those of hydroxyapatite, confirming the fabrication of hydroxyapatite particles. XPS spectrum of the HA microparticles (Fig. Ie) matched previously reported hydroxyapatite XPS spectrum [22]. The Ca/P values were calculated directly from XPS data and were on average 1.36 +/− 0.08. Finally, HAp were suspended, alongside MSCs in a collagen gel, and co-cultured for 24h. Gels containing cells but no HA were used as a control. Brightfield images of the gels (Image IIb.) showed that while HAp seemed well uniformly distributed throughout the gel, SBp aggregated and formed larger structures (black). Live/Dead assay was performed on the scaffolds after 24h of incubation (Fig. IIa), where green represents viable cells and red stains dead cells. The image displays high cell viability after encapsulation of the cells and microparticles in scaffolds. With 100% of cells stained green in all groups, viability was not affected by the incorporation of HAp.

Osteogenic potential of Calcium Deficient Hydroxyapatite Microparticles (CDHAp)

Cells were isolated from the collagen scaffolds after 14 days of in vitro culture, and DNA was collected. The quantification of DNA showed no significant difference between groups at day 0. After 14 days of culture in osteogenic media, a significantly lower ($p<0.05$) DNA concentration in the samples containing CDHAp compared to the samples containing SBp or no HA (Figure IIIa) was found. However, XTT results (normalized to DNA content) showed a significantly increased metabolic activity (p,0.05) at D14 for the cells cultured with CDHAp when compared to the two other groups (Figure IIIb). Osteogenic differenciation was observed by quantifying mRNA expression of BMP2 and OCN. Rt-PCR results showed an upregulation in gene expression of BMP2 and OCN in MSCs cultured with both HAp (CDHAp and SBp) after 14 days (Figure IIIc). A significant increase in fold change ($p<0.05$) in mRNA of both osteogenic markers was observed in the CDHAp group. Histological images of collagen scaffolds cultivated for 14 days and stained with Von Kossa are shown in Figure IIId. Mineralization, seen in dark brown/black, was minimal in no HA culture groups on day 14 and appeared the most intense in CDHAp groups.

VEGF encapsulation and Bioactivity of CDHAp

Synthesized calcium deficient hydroxyapatite particles can be very efficient drug vehicle thanks to their high drug loading. To demonstrate these advantages, the drug loading and release of CDHAp have been evaluated. Figure Iva shows the drug loading efficiency of both CDHAP and SBp. The CDHAp showed a high VEGF loading efficiency of 64.88 +/− 4.82 %, which was significantly higher than the loading efficiency of SBp ($p<0.05$). The sustained release of VEGF from the HA particles into PBS was investigated. A burst of about 40% (1557 pg/ml) of VEGF from CDHAp was observed during the first 24h, followed by a more linear and gradual release over the following 14 days, during which 88% (3425 pg/ml) of the entire amount of VEGF was released. Under the same condition, 80% VEGF (814 pg/ml) was release from SBp after 24h, and about 93% (946 pg/ml) of the initial VEGF concentration was released after 14 days.

The angiogenic potential of CDHAp was assessed and compared to that of SBp. HUVECs were suspended in collagen gels, along with either SBp or CDHAp. Both microparticles were loading with VEGF. No HA particles were used as a control. After 7 days of in vitro culture, cells were isolated from the scaffolds and DNA was isolated. The DNA quantification assay showed no significant difference between groups at day 0. After 7 days of culture, a significantly higher DNA concentration ($p<0.05$) was found in the samples containing CDHAp compared to the samples containing SBp (Figure IVb). Similarly, XTT results (normalized to DNA content) showed a significantly increased metabolic activity (p,0.05) at D7 for the cells cultured with CDHAp when compared to the two other groups (Figure IVc). mRNA expression of PECAM and VEGF was also used to monitor angiogenesis. Rt-PCR showed an increase in gene expression of both PECAM and VEGF in HUVECs cultured with both HAp (CDHAp and SBp) after 7 days (Figure IVd). A significant increase in fold change in mRNA of both angiogenic markers ($p<0.05$) was observed in the CDHAp group. The ability of VEGF-CDHAp to stimulate the migration of HUVECs was investigated (Fig. IVe). HUVEC migratory activity when cultured with CDHAp increased when compared to SBp. Quantification of the invaded area indicated that wound closure was significantly higher ($p<0.05$) when HUVECS were supplemented with CDHAp rather than SBp.

Discussion

The first objective was to develop microparticles and characterize their size, chemical properties, and Ca/P ratio to validate the formation of hydroxyapatite. Hydroxyapatite particles (HAp) were synthesized in a two-step reaction. We used aspartic acid and sodium dodecyl sulfate as a surfactant to form hollow calcium carbonate (CaCO3) template. HA was then formed by an anion exchange between CaCO3 and disodium phosphate dodecahydrate (Na2HPO4, 12H2O) under constant stirring (Figure Ia). SEM images showed that HAp particles, unlike SBp, had a coarse surface, constructed by short needle nanoparticles (276nm by 20nm), creating numerous interstitial spaces, or mesopores, which is believed to improve the absorption of growth factors. The particles composition was validates using XPS and XRD. In addition to the normal Ca, P and O peaks, a C (1s) peak was observed in the XPS spectrum. Carbonate is an impurity commonly found into a variety of synthetic calcium phosphates. The Ca/P values calculated using XRD were on average 1.36 +/− 0.08. Stoichiometric hydroxyapatite has a Ca/P ration of 1.67, indicating that the HAp are calcium deficient. Bone is actually constituted of nano-crystalline, non-stoichiometric, calcium-deficient apatites whose Ca/P molar ratio can go from 1.33 up to 1.67 [23]. Structurally and physically, they are unstable and very reactive due to a lower Ca/P ratio hence a higher solubility [24]. Several hydroxyapatite parameters can affect the cellular activity: its composition, dissolution, topography and surface energy. For example, the dissolution rate of HA has been linked to early bone formation in vivo and the osteogenic differentiation in vitro, suggesting that free calcium and inorganic phosphates can have a positive effect on bone formation [25]. Osteoblasts have also been shown to be responsive to the crystal shape: larger apatite crystals can an increase in bone sialoprotein and osteocalcin expression after 3 weeks of culture [26]. This would suggest that the CDHA particles, presenting a similar

composition and structure than natural bone mineral, could be of greater biological interest than stoichiometric, commercially available HA [27], [28].

Osteoblastic differentiation of hMSCs encapsulated in collagen with either CDHAp or SBp was assessed and compared to that of hMSCs in collagen only to determine the effect of the microparticles. The results suggest that hMSCs cultured with CDHAp were less proliferative but more differentiated than hMSCs grown with SBp. Research suggests that proliferation and differentiation are correlated: differentiation usually correspond to a stop in proliferation [30], [31]. In addition, Shum *et al.* demonstrated that metabolic activity is increased during osteogenic differentiation of MSCs [32]. Active oxidative phosphorylation is likely needed to meet the high energy demand needed for the production of extracellular matrix protein during osteogenesis. Both BMP2 and OCN are late marker of osteogenesis and their expression coincide with matrix mineralization and is at its maximum after 21 days post osteogenic induction [33]. Therefore it would appear that MSCs grown with CDHAp are at a later stage of osteogenesis. In addition, during osteogenic differentiation, hMSCs will increase their deposition of minerals in the extracellular matrix (ECM). Von Kossa staining was performed to study the mineralization and calcification of the collagen scaffolds, indicative of the stage of osteoblastic differentiation. Using evidence from cellular metabolic activity and gene expression results as well as Von Kossa staining, we can conclude that overall, the coculture of hMSCs with CDHAp resulted in greater lineage commitment toward osteogenic differentiation, compared to control and SBp. Additionally, this suggests that calcium deficient hydroxyapatite is more biologically relevant and improve osteogenesis when compared to hydroxyapatite.

To demonstrate the advantages of using HAp, the drug loading and release capabilities of CDHAp were evaluated. The CDHAp showed a high VEGF loading efficiency suggesting that the inner hollow space and the mesoporous structures at the surface of CDHAp plays an major role in increasing the specific surface area, and therefore enhancing the loading efficiency. Because the initial concentration was high, the absorption of VEGF onto the HAp was primalry obtained through ionic affinity. VEGF was then able to diffuse in between the needle-like crystals on the surface of the microparticles and be stored into the hollow space in the center. The sustained release of growth factors from the microparticles was investigated. A burst of about 40% of VEGF from CDHAp was observed during the first 24h, followed by a more gradual and linear release over the following 14 days. Under the same condition, 80% VEGF was release from SBp after 24h. Compared to SBp, CDHAp hollow core could also slow down the drug release and attenuating the initial burst release of VEGF. The hollow interior could serve as a reserve of drug, maintaining a constant release rate. Comparing the release rates of CDHAp with SBp, CDHAp released their cargo much slower than SBp, which prolong the drug's effect. Finally, the angiogenic potential of the loaded CDHAp was evaluated. A significant increase in metabloic activity, upregulation of angiogenic genes and migratory acitivity was observed in cells grown with CDHAp. Altogether, these results indicate the superior ability of CDHAp loaded with VEGF to promote angiogenesis.

Conclusion

This study demonstrated the successful fabrication of calcium deficient hydroxyapatite microparticles, with biological properties closer to the bone than stoichiometric, commercially available hydroxyapatite. This CDHAP exhibit a well-defined 3D network of crystalline nanoplates forming mesoporous and hollow structures. The high specific area created by those structures enabled the loading of VEGF with high efficiency when compared to the loading efficiency of SBp. The high loading efficiency and sustained drug release property combined with our in vitro experiment results indicate that VEGF-CDHAp can be used to improve both osteogenesis and angiogenesis in vitro. The particles developed in this study could be used to deliver not only VEGF but multiple growth factors or other relevant bioactive factors and could have many applications in bone tissue engineering where the sustained release of factors is necessary.

References

[1]. Novosel EC, Kleinhans C, and Kluger PJ, “Vascularization is the key challenge in tissue engineering,” Adv. Drug Deliv. Rev, vol. 63, no. 4–5, pp. 300–311, 4. 2011. [PubMed: 21396416]

[2]. Ferrara N and Gerber HP, “The role of vascular endothelial growth factor in angiogenesis.,” Acta Haematol, vol. 106, no. 4, pp. 148–56, 2001. [PubMed: 11815711]

[3]. Iruela-Arispe ML and Dvorak HF, “Angiogenesis: a dynamic balance of stimulators and inhibitors.,” Thromb. Haemost, vol. 78, no. 1, pp. 672–7, 7. 1997. [PubMed: 9198237]

[4]. SILVA EA and MOONEY DJ, “Spatiotemporal control of vascular endothelial growth factor delivery from injectable hydrogels enhances angiogenesis,” J. Thromb. Haemost, vol. 5, no. 3, pp. 590–598, 3. 2007. [PubMed: 17229044]

[5]. Marui A et al., “Simultaneous application of basic fibroblast growth factor and hepatocyte growth factor to enhance the blood vessels formation,” J. Vasc. Surg, vol. 41, no. 1, pp. 82–90, 1. 2005. [PubMed: 15696049]

[6]. Epstein NE, “Complications due to the use of BMP/INFUSE in spine surgery: The evidence continues to mount.,” Surg. Neurol. Int, vol. 4, no. Suppl 5, pp. S343–52, 2013. [PubMed: 23878769]

[7]. Richardson TP, Peters MC, Ennett AB, and Mooney DJ, “Polymeric system for dual growth factor delivery,” Nat. Biotechnol, vol. 19, no. 11, pp. 1029–1034, 11. 2001. [PubMed: 11689847]

[8]. Chen RR and Mooney DJ, “Polymeric growth factor delivery strategies for tissue engineering.,” Pharm. Res, vol. 20, no. 8, pp. 1103–12, 8. 2003. [PubMed: 12948005]

[9]. Kirby GTS et al., “Microparticles for Sustained Growth Factor Delivery in the Regeneration of Critically-Sized Segmental Tibial Bone Defects.,” Mater. (Basel, Switzerland), vol. 9, no. 4, 3. 2016.

[10]. Quinlan E, López-Noriega A, Thompson EM, Hibbitts A, Cryan SA, and O’Brien FJ, “Controlled release of vascular endothelial growth factor from spray-dried alginate microparticles in collagen-hydroxyapatite scaffolds for promoting vascularization and bone repair,” J. Tissue Eng. Regen. Med, vol. 11, no. 4, pp. 1097–1109, 4. 2017. [PubMed: 25783558]

[11]. Bose S, Tarafder S, Edgington J, and Bandyopadhyay A, “Overview Biomaterials for regenerative medicine Calcium phosphate Ceramics in drug delivery.”

[12]. de Groot K, Bioceramics of Calcium Phosphate. CRC Press, 2018.

[13]. Rey C, “Calcium phosphate biomaterials and bone mineral. Differences in composition, structures and properties.,” Biomaterials, vol. 11, pp. 13–5, 7. 1990.

[14]. LeGeros RZ, “Calcium Phosphate-Based Osteoinductive Materials,” Chem. Rev, vol. 108, no. 11, pp. 4742–4753, 11. 2008. [PubMed: 19006399]

[15]. Bandyopadhyay A, Bernard S, Xue W, and Bose S, “Calcium Phosphate-Based Resorbable Ceramics: Influence of MgO, ZnO, and SiO2 Dopants,” J. Am. Ceram. Soc, vol. 89, no. 9, pp. 2675–2688, 8. 2006.

[16]. Doonan S, “Chromatography on Hydroxyapatite,” in Protein Purification Protocols, New Jersey: Humana Press, pp. 191–194.

[17]. Dubok VA, “Bioceramics — Yesterday, Today, Tomorrow,” Powder Metall. Met. Ceram, vol. 39, no. 7/8, pp. 381–394, 2000.

[18]. Feng D, Shi J, Wang X, Zhang L, and Cao S, “Hollow hybrid hydroxyapatite microparticles with sustained and pH-responsive drug delivery properties,” RSC Adv, vol. 3, pp. 24975–24985, 2013.

[19]. Wang K et al., “Sustained release of simvastatin from hollow carbonated hydroxyapatite microspheres prepared by aspartic acid and sodium dodecyl sulfate,” Mater. Sci. Eng. C, vol. 75, pp. 565–571, 6. 2017.

[20]. Liang C-C, Park AY, and Guan J-L, “In vitro scratch assay: a convenient and inexpensive method for analysis of cell migration in vitro,” Nat. Protoc, vol. 2, no. 2, pp. 329–333, 2. 2007. [PubMed: 17406593]

[21]. Patel DB, Gray KM, Santharam Y, Lamichhane TN, Stroka KM, and Jay SM, “Impact of cell culture parameters on production and vascularization bioactivity of mesenchymal stem cell-derived extracellular vesicles.,” Bioeng. Transl. Med, vol. 2, no. 2, pp. 170–179, 2017. [PubMed: 28932818]

[22]. † Lu Hongbo B., ‡ Campbell Charles T., † and Graham Daniel J., and § Ratner Buddy D.†, “Surface Characterization of Hydroxyapatite and Related Calcium Phosphates by XPS and TOF-SIMS,” 2000.

[23]. Mavropoulos E, Rossi AM, da Rocha NCC, Soares GA, Moreira JC, and Moure GT, “Dissolution of calcium-deficient hydroxyapatite synthesized at different conditions,” Mater. Charact, vol. 50, no. 2–3, pp. 203–207, 3. 2003.

[24]. Lin JHC, Kuo KH, Ding SJ, and Ju CP, “Surface reaction of stoichiometric and calcium-deficient hydroxyapatite in simulated body fluid,” J. Mater. Sci. Mater. Med, vol. 12, no. 8, pp. 731–741, 2001. [PubMed: 15348246]

[25]. Barrère F, van Blitterswijk CA, and de Groot K, “Bone regeneration: molecular and cellular interactions with calcium phosphate ceramics.,” Int. J. Nanomedicine, vol. 1, no. 3, pp. 317–32, 2006. [PubMed: 17717972]

[26]. CHOU Y, HUANG W, DUNN J, MILLER T, and WU B, “The effect of biomimetic apatite structure on osteoblast viability, proliferation, and gene expression,” Biomaterials, vol. 26, no. 3, pp. 285–295, 1. 2005. [PubMed: 15262470]

[27]. Suzuki O et al., “Bone formation enhanced by implanted octacalcium phosphate involving conversion into Ca-deficient hydroxyapatite,” Biomaterials, vol. 27, no. 13, pp. 2671–2681, 5 2006. [PubMed: 16413054]

[28]. Dorozhkin SV, “A review on the dissolution models of calcium apatites,” Prog. Cryst. Growth Charact. Mater, vol. 44, no. 1, pp. 45–61, 1. 2002.

[29]. Oryan A, Kamali A, Moshiri A, and Baghaban Eslaminejad M, “Role of Mesenchymal Stem Cells in Bone Regenerative Medicine: What Is the Evidence?,” Cells Tissues Organs, vol. 204, no. 2, pp. 59–83, 2017. [PubMed: 28647733]

[30]. Strehl R, Schumacher K, and Minuth WW, “Proliferating Cells versus Differentiated Cells in Tissue Engineering,” 2002.

[31]. Ruijtenberg S and van den Heuvel S, “Coordinating cell proliferation and differentiation: Antagonism between cell cycle regulators and cell type-specific gene expression.,” Cell Cycle, vol. 15, no. 2, pp. 196–212, 2016. [PubMed: 26825227]

[32]. Shum LC, White NS, Mills BN, de M. Bentley KL, and Eliseev RA, “Energy Metabolism in Mesenchymal Stem Cells During Osteogenic Differentiation.,” Stem Cells Dev, vol. 25, no. 2, pp. 114–22, 1. 2016. [PubMed: 26487485]

[33]. Aubin JE, “Bone stem cells.,” J. Cell. Biochem. Suppl, vol. 30–31, pp. 73–82, 1998.

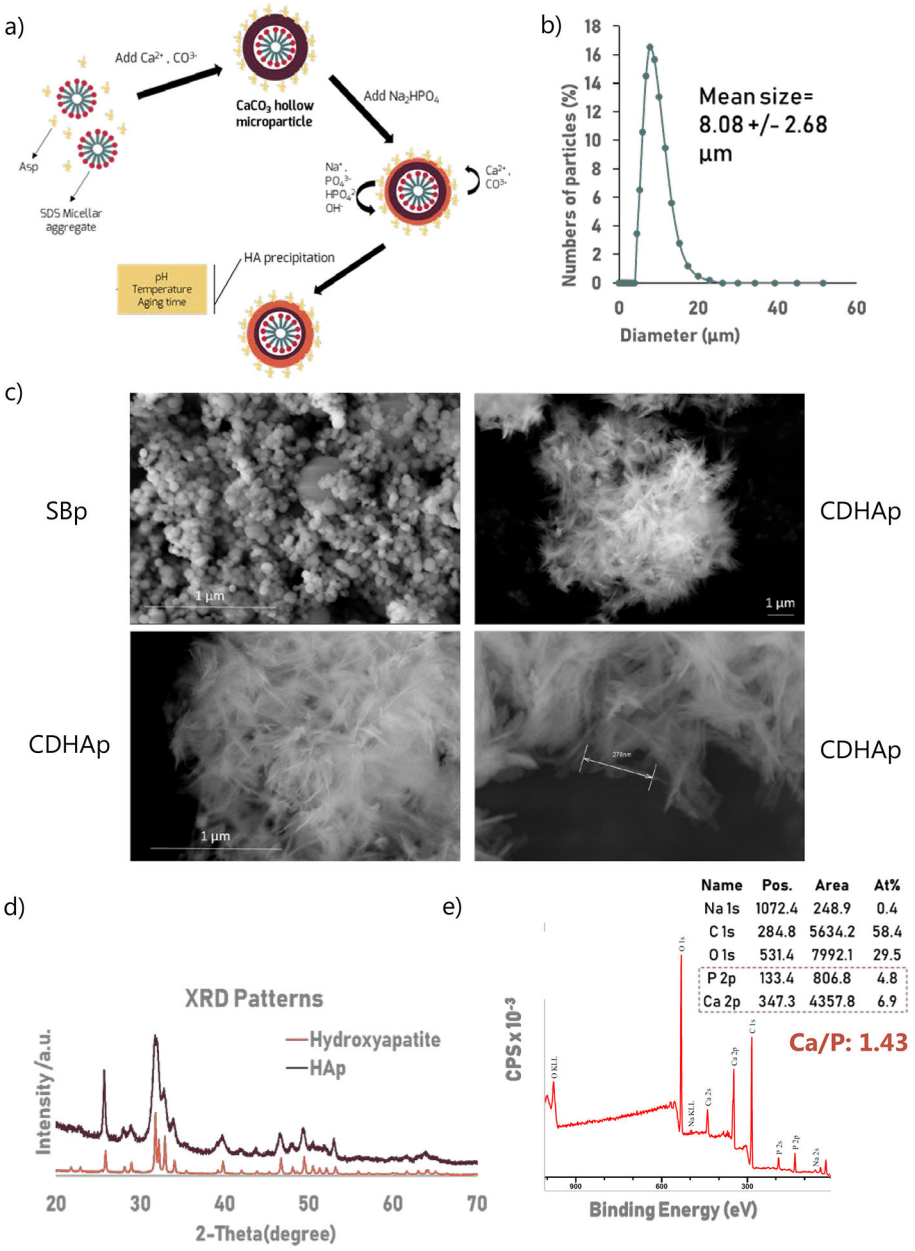

Figure I: Hydroxyapatite Particles Characterization.

Particle size distribution, XRD and XPS were performed using n=3 biological replicates. (a) Hydroxyapatite particles (HAp) were synthesized in a two-step reaction. Aspartic acid and sodium dodecyl sulfate were used as surfactant to form hollow calcium carbonate (CaCO3) template. HA was then form by an anion exchange between CaCO3 and disodium phosphate dodecahydrate (Na2HPO4, 12H2O) under constant stirring (b) Particles size distribution. Average diameter is 8.08 +/− 2.68 µm. 96.35% of particles' diameter is with the range of 5–20 µm. (c) SEM images of the particles show that homogeneous crystalloids were obtained. HAp particles, unlike SBp, had a coarse surfaces, constructed by short needle nanoparticles creating numerous interstitial spaces (d) XRD patterns of the synthesized microparticles and hydroxyapatite (PDF 01-070-4465). (e) XPS spectrum of the HA microparticles matched

previously reported hydroxyapatite XPS spectrum. Besides the expected Ca, P, and O peaks, a C (1s) peak was observed. Ca/P indicates that HAp are calcium deficient.

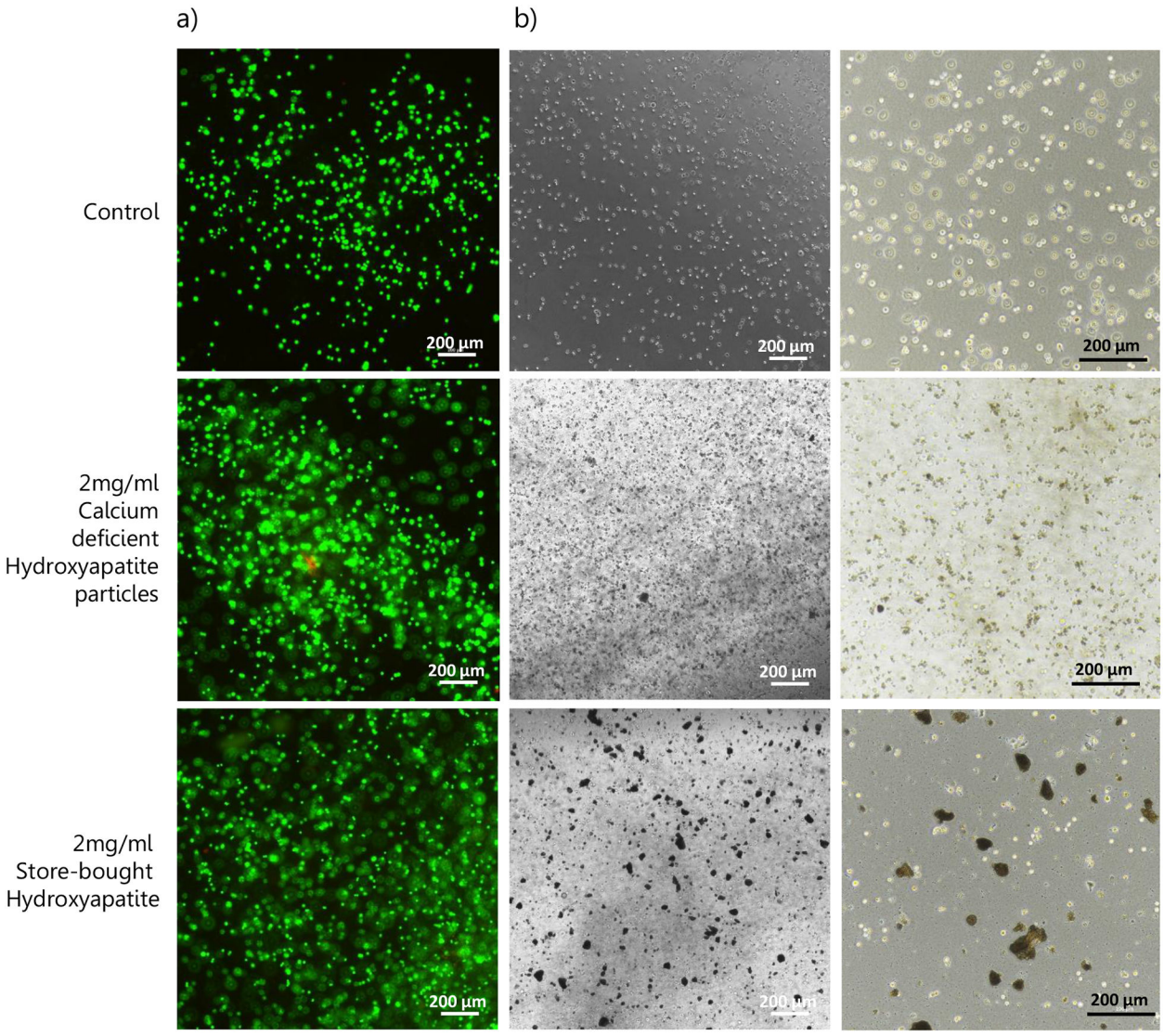

Figure II: Hydroxyapatite Particles Characterization (2).

(a) Cell viability after 24h of culture with either HAp or SBp. Green represents viable cells and red stains dead cells. The image displays high cell viability after encapsulation of the cells and microparticles in scaffolds. (b) Brightfield images of the gels showed that while HAp seemed well uniformly distributed throughout the gel, SBp aggregated and formed larger structures (black).

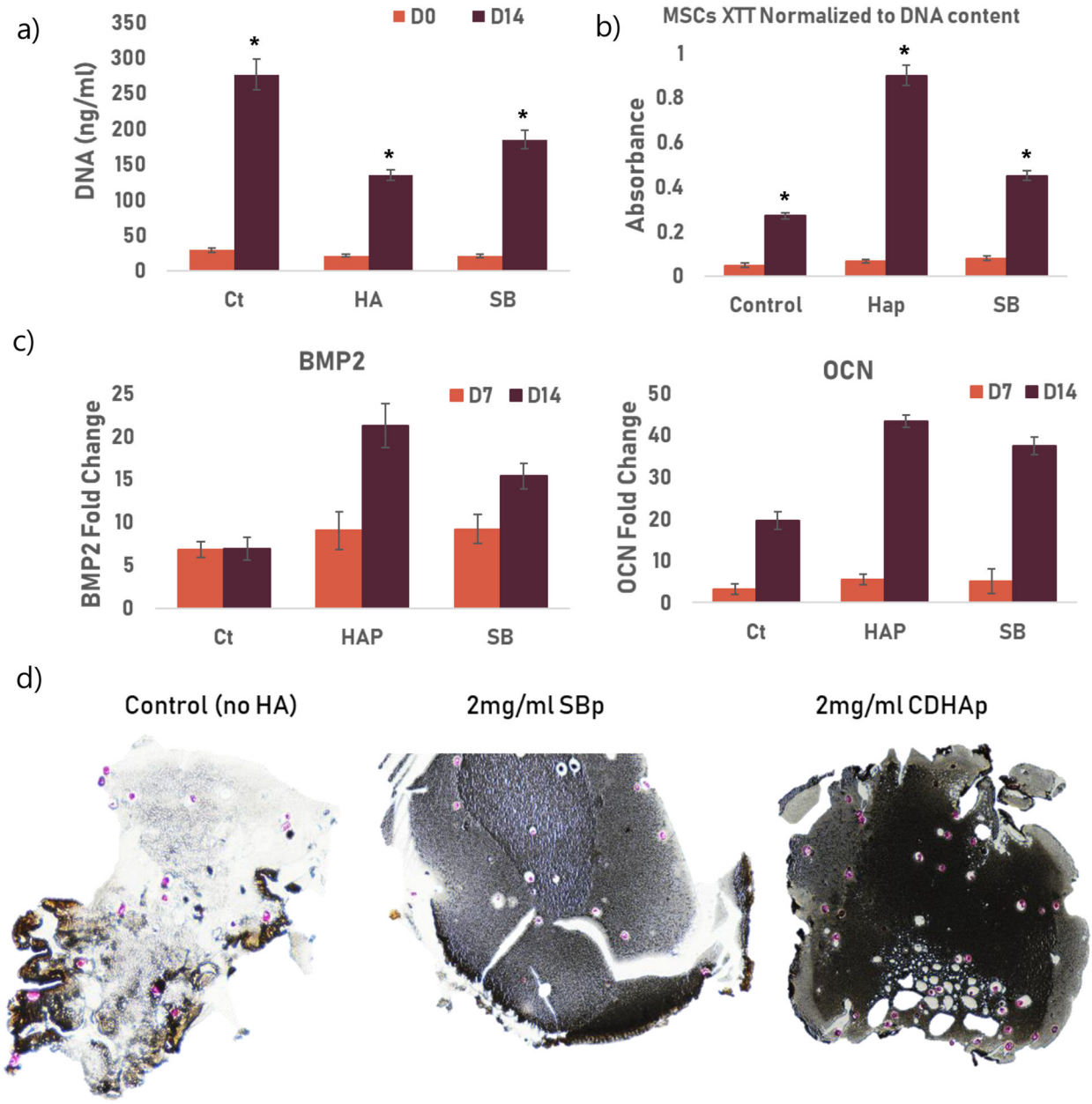

Figure III: Osteogenic Potential of CDHAp.

Ct: control group, HAp: 2ml/ml CDHAp and SB: 2mg/ml commercially available HA (Sigma).) * indicated a statistical difference between groups. All experiments were performed using biological triplicates and technical triplicates (n=9) (a) After 14 days of culture in osteogenic media, a significantly lower ($p<0.05$) DNA concentration in the samples containing CDHAp compared to the samples containing SBp or no HA (b) Metabolic activity of cells after 0 and 14 days of culture. The results are normalized to DNA content. Results showed a significant increase ($p<0.05$) in metabolic activity at D14 in the CDHAp group. (c) mRNA fold change for BMP2 and OCN after 7 and 14 days of culture. Rt-PCR showed an increase in gene expression of BMP2 and OCN in MSCs cultured with

both HAp (CDHAp and SBp) after 14 days (d) Von Kossa histology staining shows great calcification (black) in SBHAp cells on Day 14 compared to SBp. Cells are stained pink.

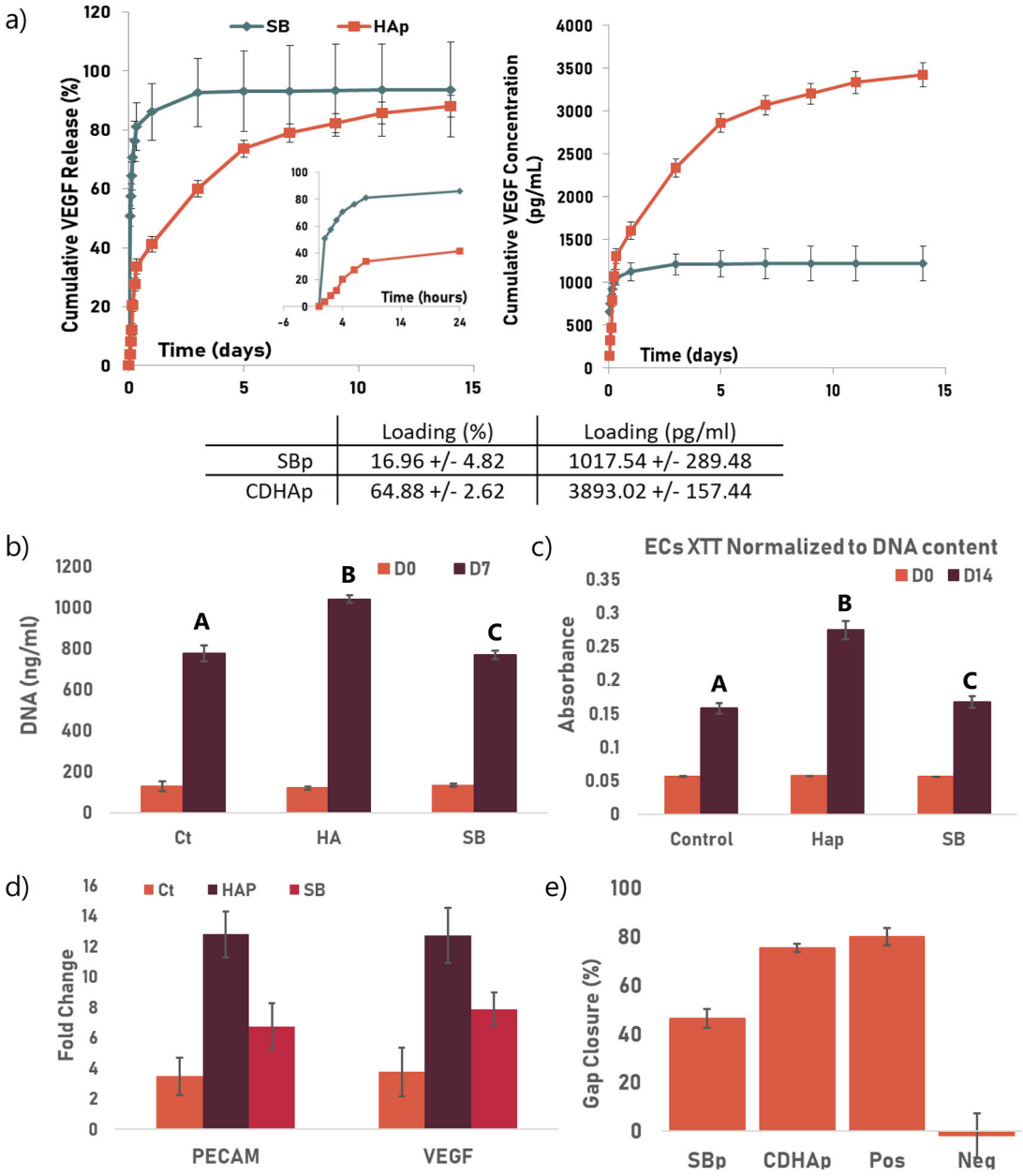

	Loading (%)	Loading (pg/ml)
SBp	16.96 +/- 4.82	1017.54 +/- 289.48
CDHAp	64.88 +/- 2.62	3893.02 +/- 157.44

Figure IV: VEGF Release and CDHAp Bioactivity.

Ct: control group, Hap: HA: 2ml/ml CDHAp and SB: 2mg/ml commercially available HA (Sigma). Groups not sharing a letter are statistically different. All experiments were performed using biological triplicates and technical triplicates (n=9) (a) Release profile of VEGF from SBp and CDHAp. The insert in the first graph shows the first 24h of release. The table summarize the loading efficiency for both particles. (b) DNA quantification after 0 and 7 days of culture. After 7 days of culture, a significantly higher DNA concentration ($p<0.05$) was found in the samples containing CDHAp compared to the samples containing SBp (c) XTT results (normalized to DNA content) showed a significantly increased metabolic activity ($p<0.05$) at D7 for the cells cultured with CDHAp when compared to the two other groups (d) mRNA expression of PECAM and VEGF was also used to monitor

angiogenesis. Rt-PCR showed an increase in gene expression of both PECAM and VEGF in HUVECs cultured with both HAp (CDHAp and SBp) after 7 days. A significant increase in fold change in mRNA of both osteogenic markers was observed in the CDHAp group ($p<0.05$). (e) Migration assay. Quantification of invaded area indicated that wound closure was significantly higher when HUVECS were supplemented with CDHAp rather than SBp.